Current Topics in Electrochemistry
Vol. 23, 2021

Original Article

The effect of coumaric acid on corrosion of iron

Ivana Škugor Rončević[1,*], Nives Vladislavić[1], Marijo Buzuk[1], Maša Buljac[2] and Marta Podrug[3]

[1]Department of General and Inorganic Chemistry, Faculty of Chemistry and Technology, University of Split, R. Boškovića 35, 21000 Split; [2]Department of Environmental Chemistry, Faculty of Chemistry and Technology, University of Split, R. Boškovića 35, 21000 Split; [3]Faculty of Chemistry and Technology, University of Split, R. Boškovića 35, 21000 Split, Croatia.

ABSTRACT

Materials like iron and its alloys (mild steel, stainless steel) are subject of longstanding technological interest for engineering applications due to many advantages. However, one of the major drawbacks is a complex anodic dissolution of iron in contact with an environment containing ionically conducting species which depends greatly upon composition and pH of the electrolyte solution, surface charge (acid-base properties of the surface), etc. The successful application of iron and its alloys relies on the formation of a surface passive layer that significantly modifies the reactivity and represents a key factor of iron protection against corrosion. The environmental restrictions put in focus the use of natural products as green corrosion inhibitors. One of four phenolic acids in natural products, propolis, which is known to possess anticorrosion efficacy for different metals and alloys, is *p*-coumaric acid. The aim of the present study is to investigate the influence of cinnamic acid derivative (*o*-coumaric acid (OKA) and *p*-coumaric acid (PKA)) films on the corrosion resistance of iron in sodium chloride solution by means of *dc* and *ac* electrochemical methods. The surface films were characterized using Fourier transform infrared spectroscopy and optical microscopy.

KEYWORDS: iron, corrosion inhibition, *o*-coumaric acid, *p*-coumaric acid, electrochemical behavior.

*Corresponding author: skugor@ktf-split.hr

INTRODUCTION

Iron alloys, especially steels, are the most important construction materials due to their high mechanical properties such as strength, ease of fabrication, abundance, and reasonable price. The major drawback for their use in engineering applications is corrosion in many media including most outdoor atmospheres [1]. Since decreasing the corrosion rate provides economic benefits, the prevention of metal corrosion has always been an important subject to be dealt with [2]. The use of corrosion inhibitors is one of the most practical methods for protection of metals in aggressive solutions [3]. Organic compounds bearing heteroatoms with high electron density such as phosphor, sulphur, nitrogen, oxygen or those containing multiple bonds which are considered as adsorption centers, are effective as corrosion inhibitors [2, 4-7]. The adsorption occurs due to the interaction of the free electronic pairs which are readily available for sharing and/or π-orbitals of inhibitor with d-orbitals of the metal atoms, in which the metal acts as an electrophile and the inhibitor acts as a Lewis base, leading to the formation of a corrosion protection film [8-12]. This protection film can act as a barrier that limits the transport of species from the bulk to the iron surface or vice-versa [13, 14]. Green chemistry, economics and waste treatment all favor the use of environmental-friendly organic inhibitors from natural sources [15-18] such as propolis, which became, nowadays, of practical interest. Propolis with the anticorrosion efficiency for various metals and alloys also has a wide range of biological

activities such as anti-bacterial, anti-inflammatory, anti-cancer and anti-oxidant. The most common compounds in Croatian propolis tested by L. Vrsalović *et al*. are *p*-coumaric acid, chrysin and pinocembrin [3]. Coumaric acid as phenolic acid meets the second condition, *i.e.*, the presence of an electron cloud on the aromatic ring, and the electronegative oxygen atom compound in aqueous medium can induce greater adsorption of the compound on the iron surface by promoting effective inhibition [8, 19]. Coumaric acid (hydroxycinnamic acid) possesses antioxidant, anti-tumor and anti-inflammatory properties. This acid is an antioxidant which is implicated in the prevention of pathologies such as colon cancer and cardiovascular diseases [20]. It has been reported that the intestinal absorption of *p*-coumaric acid *in vivo* is highly efficient [21, 22].

The aim of the present study is to investigate the corrosion resistance of unprotected and protected iron in a slightly acid NaCl solution by using *dc* and *ac* electrochemical techniques. Before examining the corrosion behavior, the iron samples were protected by creating cinnamic acid film (*o*-coumaric acid (OKA) or *p*-coumaric acid (PKA)) on the iron surface. Quantum chemical calculations were applied to probe the electronic structure parameters of the cinnamic acid derivatives. The morphology of the surface films was studied using Fourier transform infrared spectroscopy (FTIR) and optical imaging.

MATERIALS AND METHODS

The working electrode was prepared from spectroscopically pure Fe (99.999 wt.%) obtained from Goodfellow, UK. Sample for electrode, 10 mm length and 0.6 mm in diameter, was sealed into glass tube with Polirepar S so that an area of 0.283 cm^2 was exposed to the solution. Prior to each measurement, the working electrodes prepared were abraded with SiC papers of 800-2000 grit and were polished successively with Buehler® alumina suspensions of granulation ranging from 1 μm to 0.05 μm to a mirror finish. Subsequently, the working electrodes were ultrasonically cleaned with ethanol and redistilled water. All electrochemical measurements were performed at room temperature (23 ± 1°C) in a 0.5 M NaCl solution with a pH of 6.0. The supporting electrolyte was prepared by dissolving the weighed amount of analytical grade sodium chloride salt in double distilled water (18 MΩ cm). The pH of the solution was adjusted by adding the appropriate amount of HCl(aq) (c = 0.1 M). The iron samples were protected by creating cinnamic acid self-assembled film (SAM) (*o*-coumaric acid or *p*-coumaric acid) on the iron surface or by addition of 5 mL of 0.1 M coumaric acid ethanolic solution in 100 mL of NaCl electrolyte. To form the SAM of coumaric acid, the electrode was immersed in 5 mM ethanolic solution of corresponding acid (*o*-coumaric acid, OKA and *p*-coumaric acid, PKA Sigma-Aldrich, ≥ 98.5 %) at 25° C for 1 h, rinsed with distilled water and air dried. Electrochemical measurements were performed in a conventional three-electrode cell of 100 mL volume after an immersion period of 1 h. Potential time measurements have shown that the steady-state potential values were established inside this time interval. A large area platinum electrode and the Ag|AgCl|3 M KCl electrode served as the counter and reference electrode, respectively. All potentials refer to the Ag|AgCl|3 M KCl electrode (209 mV vs. SHE). Five repeated measurements were always performed as a control.

In order to characterize the electrochemical behavior of Fe electrode, cyclic voltammetry (CV) measurements were carried out with a scan rate of 1 mV s^{-1} in a potential region from -1.0 to 1.5 V vs. Ag/AgCl.

Linear polarization measurements were obtained by changing the electrode potential automatically from -15 to +15 mV vs. open circuit potential at a scan rate of 0.3 mV s^{-1}.

Impedance measurements were performed at open circuit potential (E_{OCP}) with the *ac* voltage amplitude ±5 mV in the frequency range from 10 mHz to 100 kHz. All measurements were carried out using a Solartron SI 1287 Electrochemical Interface and a Solartron SI 1255 Frequency Response Analyzer equipped with a personal computer. The experimental data were fitted using the complex non-linear least squares fit analysis software Zview [23]. The numerical values of impedance parameters were determined with a standard deviation χ^2 less than 5×10^{-4} (errors in parameter values of 1-3%), indicating that the agreement between the proposed equivalent electrical circuits (EEC) model and the

experimental data was good. Due to the frequency dispersion (mostly attributed to the 'capacitance dispersion'), the capacitor in the EEC was replaced with the constant phase element (CPE). The impedance of CPE is defined as $Z(\mathrm{CPE})=[Q(j\omega)^n]^{-1}$, where $j\omega$ is the complex variable for sinusoidal perturbations with $\omega=2\pi f$, and n is the exponent of CPE, while Q is the frequency-independent parameter of the CPE, which represents pure capacitance when n = 1 [24, 25]. Values of $0.70 < n < 1$ indicate inhomogeneities at the microscopic level at the metal|electrolyte interface (such as surface roughness, adsorbed species, etc.) [25].

Potentiodynamic measurements were performed at a sweep rate of 1 mV s^{-1}; the potential sweep started from the open circuit potential (E_{OCP}) to the cathodic and then, to the anodic side.

Molecular modeling of the coumaric acid molecules was performed using the Semiempirical program from HyperChem 6.0.3.

In order to understand the mechanism of corrosion inhibition, the adsorption behavior of coumaric acids on the metal surface must be known. For *o*-coumaric acid, the adsorption isotherm that fits the experimental results was investigated, *i.e.* the surface coverage data was fitted to different adsorption isotherms. The surface coverage was calculated from the measured values of the corrosion current densities obtained by the Stern-Geary method, measured in 0.5 M NaCl solutions of pH 6.0 and *o*-coumaric acid containing 0.5 M NaCl solutions of pH 6.0. Different concentrations of *o*-coumaric acid in the range of $1\times10^{-5} - 5 \times 10^{-3}$ M were used. OKA was applied on the electrode surface within 30 min of immersion at 21 ± 2°C under stirring with a magnetic stirrer. The surface coverage, θ, is calculated using $\theta = [(j - j_{inh}) / j] \times 100$, where j and j_{inh} are the corrosion current densities before and after the corrosion inhibition process, respectively.

The surfaces of the working electrode, unprotected and protected, were photographed using a Canon EOS 550 d digital camera in order to visualize the coumaric coating on the Fe surface. A metallurgical microscope (A 13.0908-A) with a 200× magnification was also used for more in-depth visualization of the modified surface morphology.

To test the presence of coumaric acid SAM in the surface films on Fe, the FTIR spectra were recorded on protected Fe in the 4000–650 cm^{-1} region using Horizontal Attenuated Total Reflectance (HATR) method on a Perkin-Elmer Spectrum One FT-IR spectrometer.

RESULTS AND DISCUSSION

Figure 1 shows the cyclic voltammogram of an iron in 0.5 M NaCl solution, pH 6, at room temperature recorded in the potential range from -1.0 V to +1.5 V vs. Ag/AgCl with a scan rate of 1 mV/s. Cyclic voltammogram recording was preceded by a stabilization of the electrode open circuit potential (E_{ocp}) by electrode immersion in electrolyte solution for 60 minutes.

In the forward part of the cyclic voltammogram the current density appears preferentially on the anodic side in this potential range and two more pronounced current density peaks were observed (peaks A and B in Figure 1). These two peaks correspond to the corrosion action of the electrolyte on the iron electrode; more precisely they correspond to the dissolution of iron according to the reactions [11]:

Peak A:

$$Fe + OH^- \leftrightarrows FeOH_{ads} + H^+ + e^- \quad (1)$$

$$FeOH_{ads} \rightarrow FeOH^+ + e^- \quad (2)$$

$$FeOH^+ + H^+ \leftrightarrows Fe^{2+} + H_2O \quad (3)$$

These dissolution reactions explain the abrupt increase of current density with increase in the applied potential. The current peak B corresponds to the oxidation of the Fe^{2+}(aq) ions and deposition as Fe(III) hydrated oxide, most frequently attributed to either FeOOH or $Fe(OH)_3$ [1],

Peak B:

$$Fe^{2+} + 2H_2O \rightarrow FeOOH + e^- + 3H^+ \quad (4)$$

and to the iron dissolution according to the reactions:

$$Fe + OH^- \leftrightarrows FeOH_{ads} + H^+ + e^- \quad (5)$$

$$FeOH_{ads} \rightarrow FeOH^+ + e^- \quad (6)$$

$$FeOH^+ \rightarrow FeOH^{2+} + e^- \quad (7)$$

$$FeOH^{2+} + H^+ \leftrightarrows Fe^{3+} + H_2O \quad (8)$$

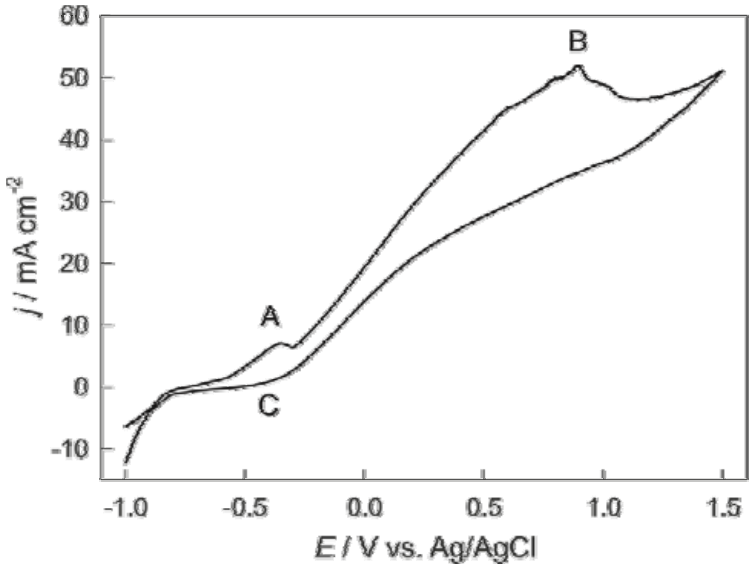

Figure 1. Cyclic voltammogram of an iron in 0.5 M NaCl solution, pH = 6, recorded with a scan rate of 1 mV/s.

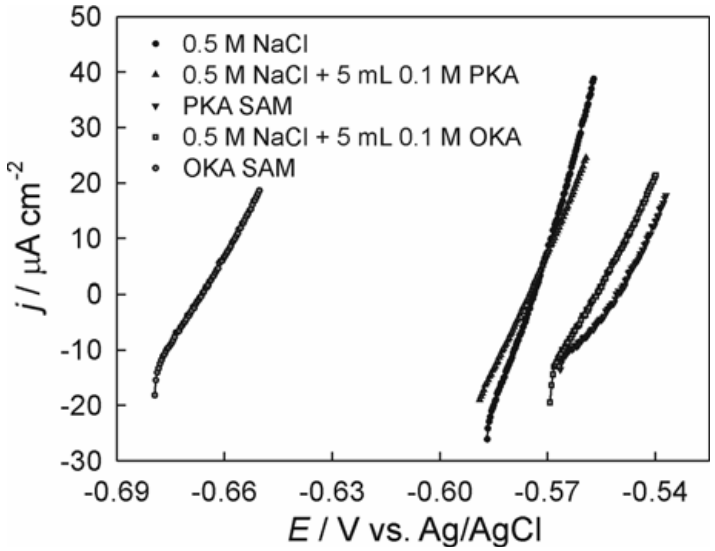

Figure 2. Linear polarization curves obtained for an iron electrode in 0.5 M NaCl solution, pH = 6, without and with the addition of coumaric acid to the solution (5 mM) or applied as a coating on Fe, recorded with a scan rate of 0.3 mV/s.

The formation of γ-FeOOH on the iron electrode is reported in the presence of Fe^{2+} ions in the electrolyte solution only at pH > 5.8 [1].

In the backward direction the cyclic voltammogram is characterized by a current density peak (peak C in Figure 1) which corresponds to the electroreduction of Fe(III) and Fe(II) iron species.

The curves shown in Figure 2 were obtained by the linear polarization method. The values of the polarization resistances, corrosion potentials and corrosion current densities are shown in Table 1, along with the calculated values of corrosion inhibition efficiency. Measurements were performed in a narrow corrosion potential range with a scan

Table 1. Values of corrosion potentials, polarization resistances and corrosion current densities obtained by Stern-Geary method for iron electrode in 0.5 M NaCl solution, pH = 6, without and with addition of coumaric acid to the solution (5 mM) or applied as a coating on Fe.

	$-E_{corr.}$ / mV	R_p / Ω cm^2	$j_{corr.}$ / μA cm^{-2}	η/ %
Fe	574	506	51.51	/
Fe_*ads_PKA	575	704	37.04	28
Fe_**SAM_PKA	550	945	27.60	46
Fe_*ads_OKA	557	880	29.63	43
Fe_**SAM_OKA	666	965	27.03	48

*ads: for values measured for an iron electrode in 0.5 M NaCl solution, pH = 6, with the addition of coumaric acid to the solution (5 mM).
**SAM: for values measured for an iron electrode in 0.5 M NaCl solution, pH = 6, with the coumaric acid applied as a coating on Fe.

rate of 0.3 mV/s. The film efficiency (inhibition efficiency) of a certain coumaric acid as a potential iron corrosion inhibitor in 0.5 M NaCl solution was determined using the expression:

$$\eta / \% = (R_{p,p} - R_{p,unp}) / R_{p,p} \quad (9)$$

wherein:

$R_{p,p}$ - the polarization resistance value for the protected iron electrode

$R_{p,unp}$ - the polarization resistance value for an unprotected iron electrode.

From the above results (Figure 2, and Table 1) it can be concluded that the addition of coumaric acid is beneficial to the corrosion resistance of iron *i.e.* increase in the slope of the polarization curve. The highest corrosion resistance has electrode on which the *o*-coumaric acid coating was applied by the self-assembled method.

Impedance measurements on the iron electrode in a 0.5 M NaCl solution, pH = 6, in the absence and with the addition of coumaric acid to the solution (5 mM) or applied as a coating on Fe were conducted. To ensure complete characterization of the interface and surface processes, the electrochemical impedance spectra were recorded in a wide frequency range (from 100 kHz to 10 mHz) with *ac* amplitude of 5 mV and at room temperature as shown in Figure 3. The results are presented in the form of Nyquist and Bode plots. Nyquist plot represents the dependence of the imaginary impedance component (Z_{imag}) on the real impedance component (Z_{real}), and Bode plot represents the dependence of the logarithm of the absolute value of the total impedance (log|Z|) and the phase angle (θ) on the logarithm of the frequency (log$f$). In all cases the obtained Nyquist plot shows depressed capacitive semicircle loops whose diameter is equal to the polarization resistance, while in the Bode plot the slopes of the log$Z$ against log$f$ curves are not -1 (often referred to as frequency dispersion) which indicates the inhomogeneities of the solid surfaces [26]. A capacitive loop in the Nyquist diagram also suggests that the corrosion of iron in base electrolyte (0.5 M NaCl, pH = 6) is mainly controlled by charge transfer process [27]. The value of the polarization resistance is an indicator of corrosion resistance that is inversely proportional to the corrosion rate. From the Bode plots it can be seen that addition of coumaric acid increases the phase angles and shifts their peaks to lower frequencies. The broadening and the shift to lower frequencies of the phase angle maxima indicate the adherence of the inhibitor to the metallic surface and the formation of inhibitor molecule protective film which smoothen the electrode surface [18]. Impedance spectra were analyzed by equivalent electrical circuits (EEC) shown in Figure 4. The equivalent circuit A (Figure 4 A) consists of resistor, R_{el} (uncompensated electrolyte resistance) in series with the parallel combination of constant phase element, CPE_1 (Q_1) and resistor, R_1 in series with the parallel combination of constant phase element,

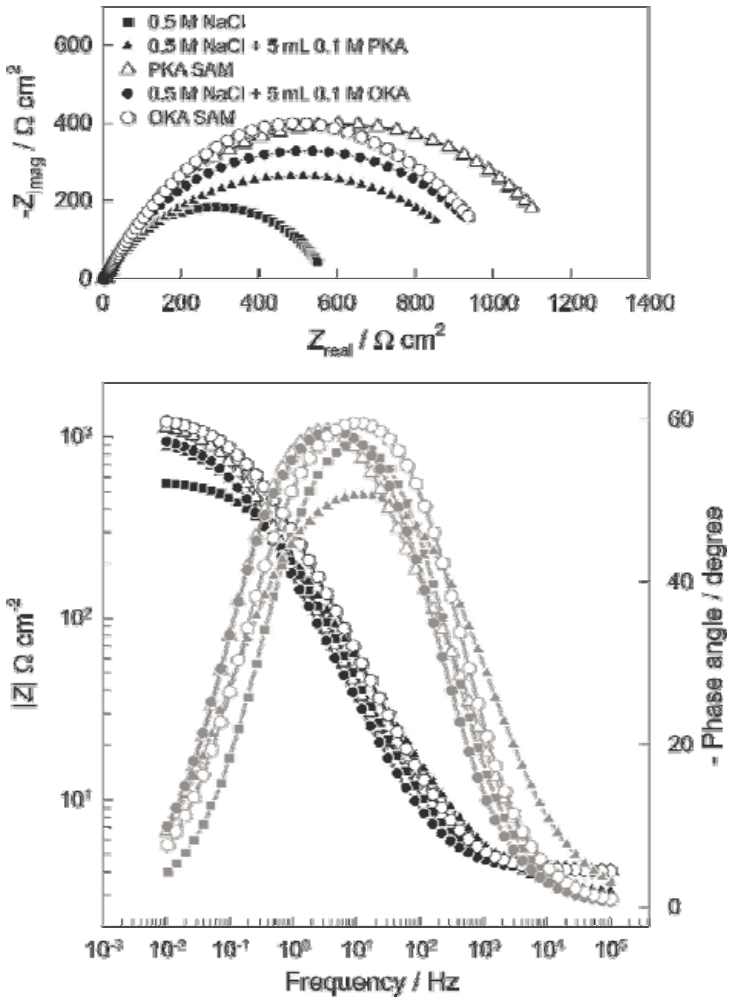

Figure 3. Nyquist and Bode plots of an iron electrode recorded in 0.5 M NaCl, pH = 6, at open circuit potential (E_{ocp}) without and with the addition of coumaric acid to the solution (5 mM) or applied as a coating on Fe.

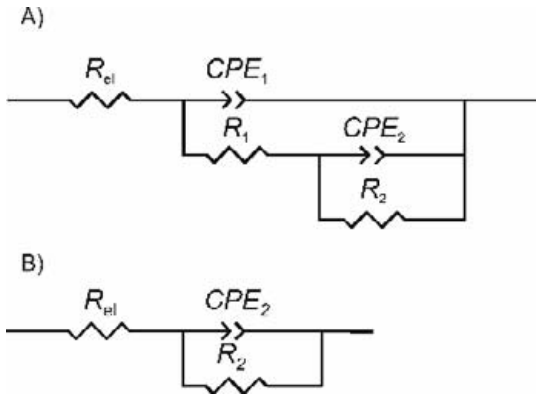

Figure 4. Equivalent electric circuits used to fit impedance data.

CPE_2 (Q_2) and resistor, R_2. The constant phase element (CPE_1) is attributed to the double layer capacitance and R_1 to the charge transfer resistance. CPE_2 and R_2 represent the film capacitance and resistance of the ion traveled through the film. The corresponding values of EEC elements obtained by fitting procedure are listed in Table 2. In addition, the inhibition efficiency calculated from R_p data ($R_p = R_1 + R_2$) are in good agreement with those obtained from polarization measurements.

From the data given in Table 2 it can be seen that the polarization resistance of the electrode increases by the addition of coumaric acid either to the base electrolyte (0.5 M NaCl, pH = 6) or as

Table 2. The inhibition efficiency (η %) and optimal values of the equivalent circuit parameters with the fitting of the impedance spectra of iron electrodes in 0.5 M NaCl, pH = 6, at open circuit potential (E_{ocp}) without and with the addition of coumaric acid to the solution (5 mM) or applied as a coating on Fe.

	$10^4 \times Q_1$ / $\Omega^{-1}cm^{-2}s^n$	n_1	R_1 / Ωcm^2	$10^4 \cdot \times Q_2$ / $\Omega^{-1}cm^{-2}s^n$	n_2	R_2 / $k\Omega cm^2$	η / %
Fe	11.08	0.725	567	/	/	/	/
Fe_ads_PKA	13.28	0.618	993	/	/	/	43
Fe_ads_OKA	14.99	0.720	1030	/	/	/	45
Fe_SAM_PKA	7.39	0.740	22	5.05	0.737	1189	53
Fe_SAM_OKA	6.25	0.757	100	2.65	0.523	1214	57

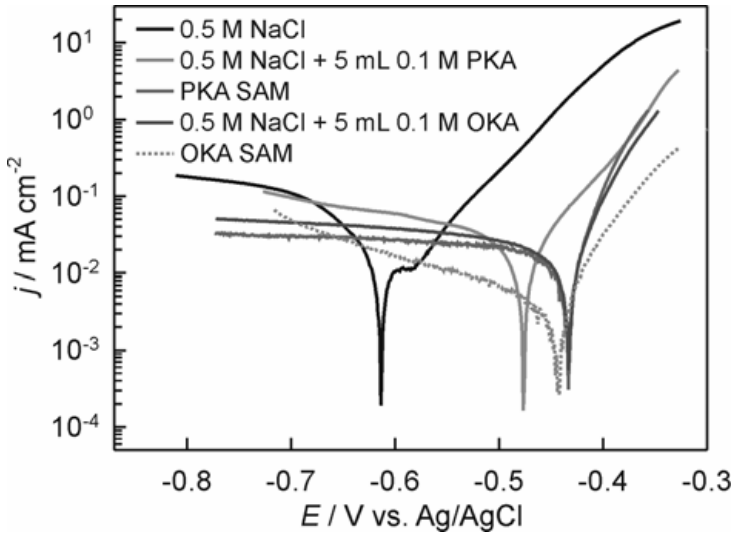

Figure 5. Potentiodynamic polarization curves obtained for an iron electrode in 0.5 M NaCl, pH = 6, without and with the addition of coumaric acid to the solution (5 mM) or applied as a coating on Fe, recorded with a scan rate of 1 mV/s.

a coating on iron. Also, the value of the constant phase element, Q_2, which is inversely proportional to the thickness of the protective film and/or the change in the dielectric constant of the surface film, decreases with the addition of coumaric acid. The inhibition efficiency of coumaric acid depends mainly on the polarization resistance rather than the constant phase element, Q_2, which may suggest that the coumaric acid molecules act by adsorption mechanism at an iron/coumaric acid interface (Table 2). Increase in the polarization resistance values could be ascribed to the effective blocking of the active sites on iron by the adsorption of inhibitor on the electrode surface, which enhances the corrosion resistance (decreases corrosion rate) of iron in NaCl solution. Thicker protective film slows the mass and charge-transfer as indicated by the high R_p and corrosion η% values. The highest η% value has electrode on which the *o*-coumaric acid coating was applied by the self-assembled method probably due to more coverage of iron surface. The values of η% are in quite good agreement with the results obtained from polarization measurements.

Figure 5 shows the Tafel representation of the polarization curves of an iron electrode in a 0.5 M NaCl solution, pH = 6, in the absence and with the addition of coumaric acid to the solution (5 mM)

or applied as a coating on Fe. Measurements were performed in a wide potential range around the open circuit potential at a scan rate of 1 mV/s and at room temperature. The values of corrosion kinetic parameters were determined by the Tafel extrapolation method: corrosion current density ($j_{corr.}$), corrosion potential ($E_{corr.}$), cathodic and anodic Tafel slope (b_c and b_a). These values are listed in Table 3.

The dissolution of iron from the electrode surface explains the abrupt increase of current with increase in the applied potential in the anodic branch. For the anodic side unprotected Fe electrode, the current increases followed by a current plateau (due to the formation of an oxide film) before abruptly increasing again till the most positive applied potential.

Both anodic and cathodic current densities as well as the $j_{corr.}$ values decrease by the addition of coumaric acid either to the base electrolyte (0.5 M NaCl, pH = 6) or as a coating on iron which is associated with a shift in $E_{corr.}$ to less negative values. These results suggest that coumaric acid behaves mainly as an anodic inhibitor (a displacement greater than 85 mV in the $E_{corr.}$ between the uninhibited and inhibited systems) which did not modify the hydrogen evolution mechanism (the reduction of H^+ ions taken place mainly through a charge transfer mechanism) yet decreased the electrode surface area available for H^+ ions [17, 28]. As seen from Figure 5, the anodic and cathodic Tafel slopes change in small range and are independent of the inhibitor application mode (the addition of coumaric acid to the base electrolyte or as a coating), indicating that the coumaric acids act as adsorptive inhibitors, *i.e*, they reduce anodic dissolution of iron at anodic sites and cathodic evolution of hydrogen at cathodic sites due to the blocking of the active reaction sites on the iron surface [11]. Table 1 shows that the maximum inhibition (lowest corrosion current density) is achieved for the electrode on which the *o*-coumaric acid coating was applied by the self-assembled method. The measurements shown in Figure 5 and the values shown in Table 3 once again confirmed the protective effect of coumaric acid on the corrosion of iron in the 0.5 M NaCl solution. It is worth mentioning that the polarization data shown in Figure 5 confirm the EIS ones in Figure 3.

The extent of adsorption of an inhibitor on the metal surface is usually influenced by the parameters such as the nature, chemical structure, distribution of charge on the molecule and charge on the metal [27, 29]. Basic information regarding the nature of interaction of the adsorbed inhibitor molecule and the iron surface can be elucidated using adsorption isotherm. The numerical values of θ for different concentrations of OKA were used in determining the isotherm, which described the best adsorption of OKA on the iron surface. Figure 6 shows that the experimental data fit best (regression coefficient of 0.989) the Flory-Huggins adsorption isotherm. Flory-Huggins isotherm equation is given by:

$$K_{ads} \times c = [\theta / (1 - \theta)] \exp(1 - n), \quad (10)$$

where n is the number of solvent molecules displaced by the inhibitor molecules, c is the inhibitor concentration, θ is the degree of coverage of the metal surface by the adsorbed inhibitor, and K_{ads} is the adsorption constant [30]. The relationship between the adsorption constant (K_{ads}) and the

Table 3. The corrosion kinetic parameters obtained for an iron electrode recorded in the 0.5 M NaCl solution, pH = 6, without and with addition of coumaric acid to the solution (5mM) or applied as a coating on Fe, v = 1 mV/s.

	$-b_c$ / mV	b_a / mV	$j_{corr.}$ / μA cm^{-2}	$-E_{corr.}$ / mV	η / %
Fe	92	55	23.21	606	/
Fe_ads_PKA	103	68	16.19	477	30
Fe_SAM_PKA	176	26	6.89	418	70
Fe_ads_OKA	162	34	9.21	418	60
Fe_SAM_OKA	188	52	4.13	433	82

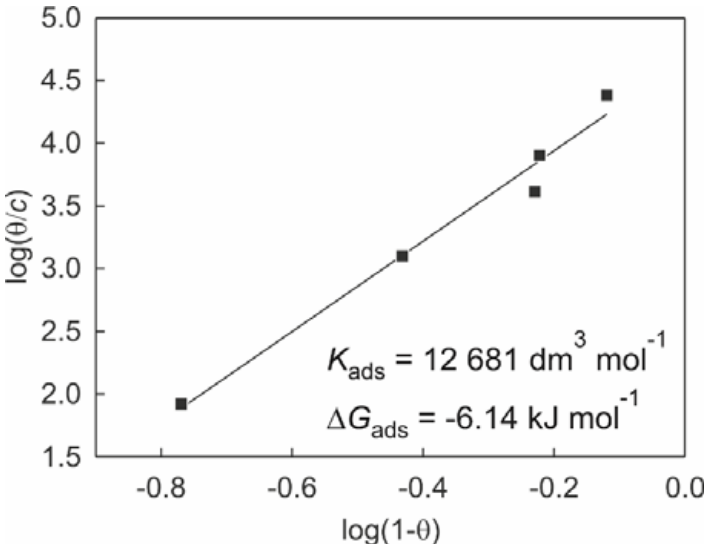

Figure 6. Flory-Huggins adsorption isotherm for iron electrode in a 0.5 M NaCl solution, pH = 6, containing *o* - coumaric acid, OKA.

Gibb free energy of adsorption (ΔG_{ads}) is given by:

$$K_{ads} = 1 / 55.5 \exp(-\Delta G_{ads} / RT), \quad (11)$$

where R is the universal gas constant, T is the absolute temperature (298 K), and 55.5 is the concentration of water in the solution in mol dm^{-3}.

The adsorption constant and Gibbs free energy were determined to be K_{ads} = 12 681 dm^3 mol^{-1} and ΔG_{ads} = -6.14 kJ mol^{-1}. The negative value of ΔG_{ads} and the higher values of K_{ads} indicate the spontaneity of adsorption process and stability of the adsorbed layer with the metal surface [12]. Generally, the values of ΔG_{ads} up to -20 kJ mol^{-1} are consistent with physisorption, while those around -40 kJ mol^{-1} involve chemisorption as a result of sharing or transfer of electrons from organic molecules to the metal surface to form a coordinate type of bond [7, 29]. In recent reports, ΔG_{ads} values in the range from -28 to -38 kJ/mol are interpreted as mixed adsorption (*i.e* both physisorption and chemisorption) [18].

The calculated adsorption value indicates that the interaction between the inhibitor molecule and metal surface is physisorption type of adsorption *i.e* adsorption of *o*-coumaric acid takes place through electrostatic interaction between the charged inhibitor molecules and charged metal surface. The relatively low value of free adsorption energy may indicate poor physical adsorption of coumaric acid on the iron electrode, which explains the obtained relatively low results for efficiency of a certain coumaric acid as a potential iron corrosion inhibitor in 0.5 M NaCl solution when coumaric acid added into the base electrolyte.

Computer modeling techniques are suitable for studying the corrosion inhibition mechanisms. To obtain qualitative information about a molecule, such as its molecular orbitals, atomic charges, or vibrational states, geometric optimizations of the coumaric acids molecules were performed using the semiempirical methods (AM1, PM3 and MNDO level). The highest occupied molecular orbital (HOMO) and the lowest unoccupied molecular orbital (LUMO) were studied. The optimized molecular structures of compounds are shown in Figure 7. The calculated quantum chemical parameters E_{HOMO}, E_{LUMO}, ΔE and μ (dipole moment) are listed in Table 4. The principle of hard and soft acid-base interaction (Hard Soft Acid Base Interaction - HSAB interaction) proposed by Pearsons is successfully applied to understand adsorption bonds and inhibitory effect. According to Pearsons, hard acids preferably react with hard bases (hard-hard interaction) while soft acids react with soft bases (soft-soft interaction) [31]. Orbital energy is a very important factor in predicting the

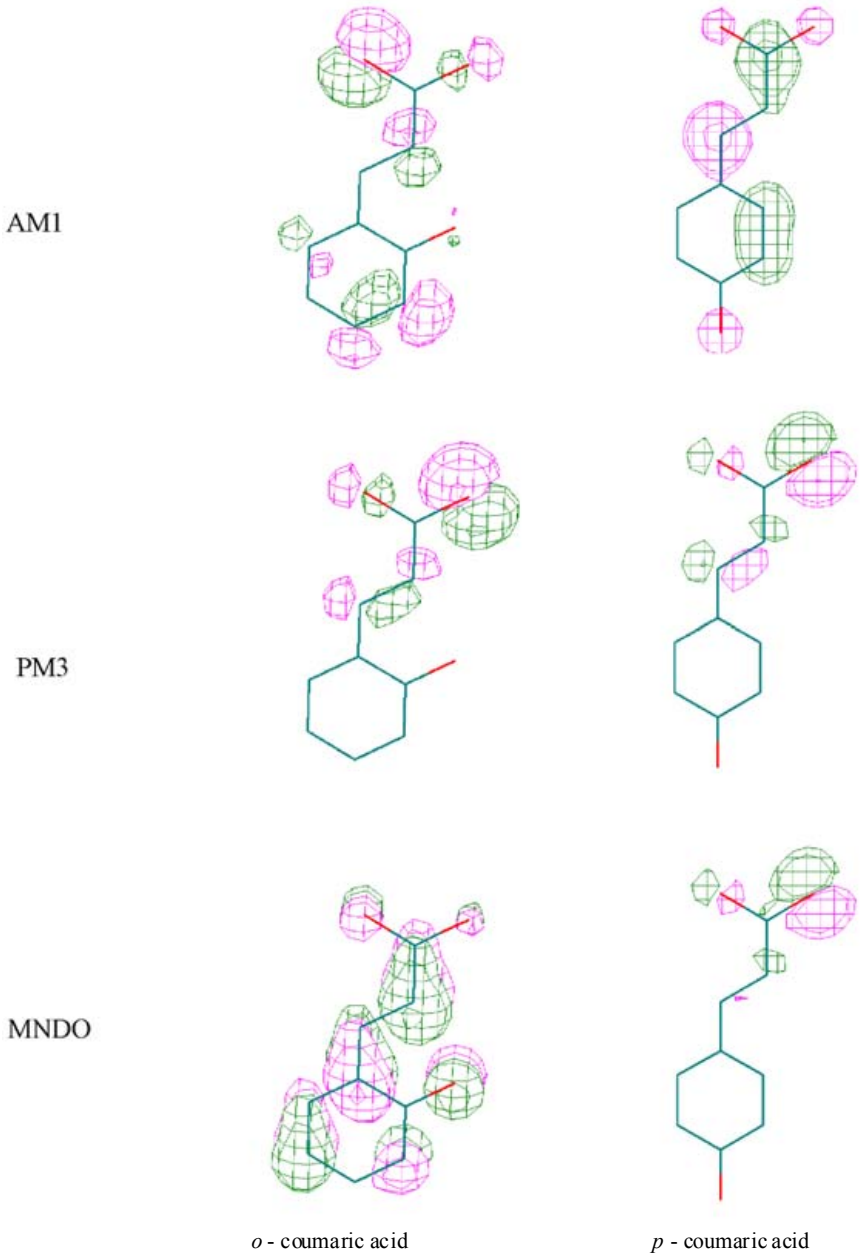

Figure 7. Geometric optimizations of coumaric acids obtained by semiempirical methods.

stability and reactivity of a molecule. The molecule with the highest value of HOMO energy will release its electrons more easily and thus will be the most reactive. On the other hand, the molecule with the lowest LUMO energy value will most easily receive electrons and thus become more reactive. According to the boundary orbital theory, high values of E_{HOMO} are associated with the ability of the inhibitor molecule to donate electrons to the metal with empty molecular orbitals [32]. The energy gap ΔE ($\Delta E = E_{HOMO} - E_{LUMO}$) is an important parameter which is related to reactivity of the inhibitor molecule toward the metal surface. The lower ΔE causes the improvement on the reactivity of the molecule, which facilitates adsorption and indicate good inhibitory efficacy [27]. Developing the HSAB model, Pearsons introduces equations for the terms chemical potential, μ, and absolute hardness, η:

$$-\mu = (I + A) / 2 = \chi \quad (12)$$

$$\eta = (I - A) / 2 \quad (13)$$

in which I represent the ionization potential and A the electron affinity. The softness of the compound, σ, is inversely proportional to its density. Chemical potential and hardness are the molecular properties of a reactant. In the acid-base reaction, *i.e* in the reaction where acid A is an electron acceptor and base B is an electron donor, the electrons will flow from the filled molecular orbital of component B to the empty molecular orbital of component A. According to Koopman's boundary orbital energy theorem,

$$-E_{HOMO} = I \quad (14)$$

$$-E_{LUMO} = A \quad (15)$$

The quantum chemical parameters of the used compounds obtained by the quantum method do not vary very significantly, meaning that the molecules will exert somewhat similar effects. From Table 4 it can be seen that the highest absolute values for E_{HOMO} and ΔE (energy gap), for all methods used, were obtained for *o*-coumaric acid, which indicates that this coumaric acid has the highest tendency to donate electrons to the empty molecular orbital of a metal as well as the best inhibitory effect. The highest population of the electron density is focused on the oxygen atoms of the carboxylic group suggesting that carboxylic oxygen atoms behave as active sites with the highest ability to interact with the metal surface.

Given the structure of the inhibitor molecule, the HOMO location is mainly distributed on the coumaric molecule and the LUMO location is distributed on the ring benzene. This indicates that electrons are transferred and accepted from the entire molecule of coumaric acid. The highest inhibition efficiency value for the electrode on which the *o*-coumaric acid coating was applied by the self-assembled method probably can be explained with the increased polarity of the *o*-coumaric acid, which results in their enhanced interaction with the charged sites on the metal surface and the enhanced adsorption probability. The polarity of the molecule (as inferred from the value of the dipole moment) which suggests a good nonspecific (the magnitude of the ΔE values > 1 eV [3]) electrostatic interaction is in good agreement with the experimental data *i.e* the inhibitor favors the physical adsorption on the metal surface [18].

The uncoated iron sample surface and iron sample surface coated with *o*-coumaric acid film were analyzed with an optical microscope. The optical image of uncoated and coated iron sample surfaces is shown in Figure 8.

From Figure 8 it can be seen that the surface is brighter indicating that the surface is covered wholly with the *o*-coumaric acid film since no pit and/or frieze (due to surface mechanical treatment) were optically observed *i.e* during the 60 minutes of immersion of the Fe electrode in the 5 mM alcoholic acid solution the acid molecules bind to the electrode surface.

FTIR analysis was performed to determine some structural characteristics as well as the presence of an *o*-coumaric acid film on the surface of the iron electrode. The FTIR spectrum of an iron sample

Table 4. Quantum chemical parameters of the used compounds obtained by the quantum method.

Method	Acid	$-E_{HOMO}$ / eV	$-E_{LUMO}$ / eV	$\lvert\Delta E\rvert$ / eV	$-\eta$ / eV	μ / D
AM1	OKA	10.873	2.440	8.433	4.217	3.987
	PKA	8.736	3.697	5.039	2.520	8.967
PM3	OKA	10.262	2.326	7.936	3.970	2.940
	PKA	9.405	2.853	6.552	3.276	1.687
MNDO	OKA	10.343	3.365	6.978	3.489	4.824
	PKA	9.032	2.710	6.322	3.161	5.920

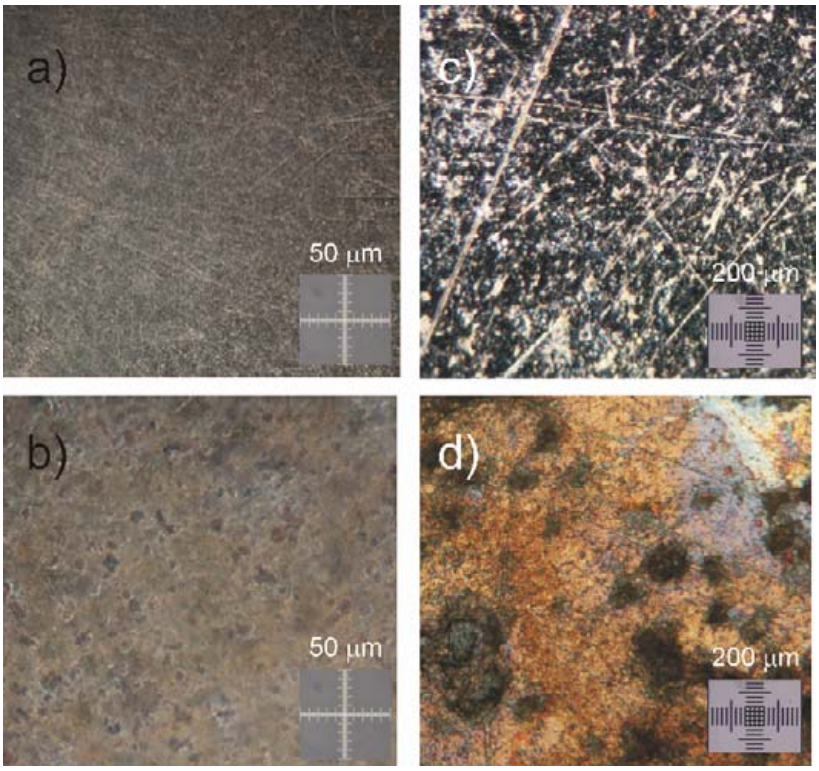

Figure 8. Optical image of uncoated iron sample surface: a) and c) and iron sample surface coated with an *o*-coumaric acid film formed by immersion of the electrode for 60 minutes in a 5 mM alcoholic acid solution: b) and d).

on which *o*-coumaric acid was applied as a coating by immersion of a Fe sample in a 5 mM alcoholic solution of *o*-coumaric acid at a temperature of 25 ^{o}C for 60 minutes was recorded. The FTIR spectrum of an *o*-coumaric acid powder (lozenge) was also recorded. The obtained spectra are shown in Figure 9.

The FTIR spectrum of the protected iron sample contains peaks which occur at very similar wavenumbers as peaks in the spectrum of OKA lozenge, which indicates that the *o*-coumaric acid film was formed on the surface of the iron sample. In the FTIR spectrum of the OKA lozenge, peaks at 1665 cm^{-1}, 1165 cm^{-1} and 974 cm^{-1} attributed to ν(C = O), ν(C – OH) and $\nu(CH)_{ar}$ stretching vibrations are visible. $\nu(CC)_{ar}$ stretching vibration was assigned to peaks visible at 1590 cm^{-1} and 1504 cm^{-1}. The vibrations of the hydroxyl group in the FTIR spectrum of the OKA lozenge, visible at 3334 cm^{-1}, 1441 cm^{-1} and 911 cm^{-1} are assigned to the ν(OH), β(OH) and γ(OH) stretching, in-plane bending and out-of-plane bending vibrations, respectively. The band at 686 cm^{-1} is assigned to the bending vibration outside the plane of the molecule, γ(CO). In the FTIR spectrum of the iron sample on which the *o*-coumaric acid film was formed, peaks can be attributed to the frequency of asymmetric COO^- stretching (1543 cm^{-1}) and the frequency of symmetric COO^- stretching (1411 cm^{-1}). The peaks at 1251 cm^{-1} and 1171 cm^{-1} are assigned to the β(CH) and ν(C–OH) stretching vibration. The broad band in the FTIR spectrum of the protected iron sample, observed in the wavenumber range of 3600–3200 cm^{-1}, was attributed to the stretching vibration of the hydroxyl group, ν(OH). The band at 941 cm^{-1} is assigned to the bending vibration outside the plane of the molecule, γ(CH)C=C [33, 34].

CONCLUSIONS

Coumaric acids added to 0.5 M NaCl solution, pH = 6, as well as applied as a coating on Fe increase the polarization resistance (linear polarization curves),

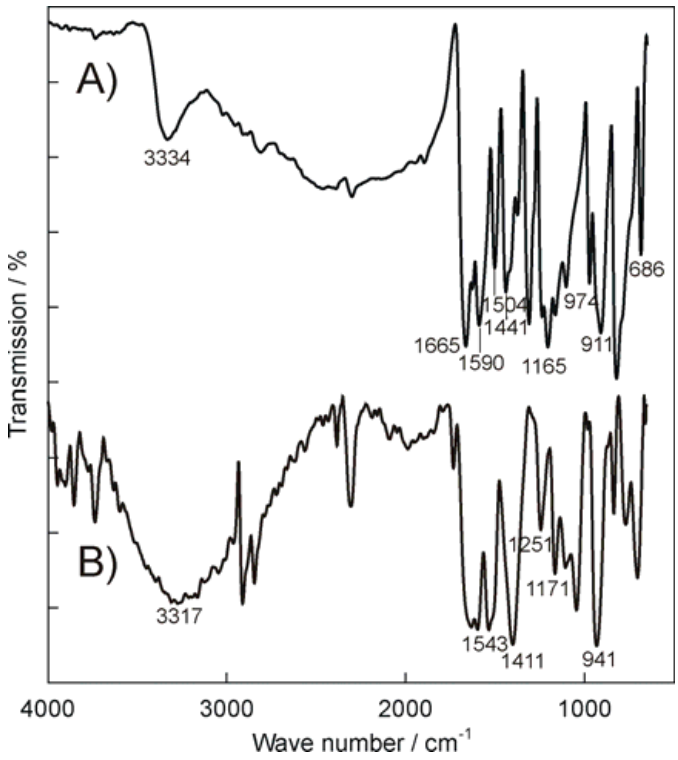

Figure 9. FTIR spectrum of A) the iron sample on which OKA is applied and B) FTIR spectrum of OKA lozenge.

then decrease the values of anodic and cathodic current density which reduces the corrosion current density and shifts the corrosion potential in the anode direction. The tested acids act as anodic corrosion inhibitors.

Experimental data obtained by impedance spectroscopy can be successfully described by selected equivalent electrical circuits. As expected, the highest polarization resistance, *i.e* the highest corrosion resistance, has the Fe electrode, on the surface of which *o*-coumaric acid is applied as a coating. The adsorption of coumaric acid can be described by the Flory-Huggins isotherm for which the calculated free adsorption energy is -29.4 kJ / mol. A value of -6.14 kJ/mol indicates the physisorption of coumaric acid molecules on the surface of the Fe electrode. All the methods used showed that coumaric acid can be successfully used as an iron corrosion inhibitor in the tested system.

The results of mathematical modeling are in accordance with the results of electrochemical measurements.

The results of FTIR analysis as well as the results obtained using an optical microscope confirm the existence of a coumaric acid film on the electrode surface.

CONFLICT OF INTEREST STATEMENT

The authors declare that there are no conflicts of interest.

REFERENCES

1. Petrović, Ž., Metikoš-Huković, M. and Babić, R. 2012, Electrochim. Acta, 75, 406.
2. Khaled, K. F., Abdel-Rehim, S. S. and Sakr, G. B. 2012, Arab. J. Chem., 5, 213.
3. Vrsalović, L., Gudić, S., Gracić, D., Smoljko, I., Ivanić, I., Kliškić, M. and Oguzie, E. E. 2018, Int. J. Electrochem. Sci., 13, 2102.
4. Quraishi, M. A. and Rawat, J. 2002, Mater. Chem. Phys., 73, 118.
5. Abd El Maksoud, S. A. 2002, Corros. Sci., 44, 803.

6. Abdallah, M. 2002, Corros. Sci., 44, 717.
7. Anand, B., Jayandran, M. and Balasubramanian, V. 2012, J. Corros. Sci. Eng., 15, 1.
8. Madkour, L. H. and Zinhome, U. A. 2010, J. Corros. Sci. Eng., 13, 1.
9. Obot, I. B., Obi-Egbedi, N. O. and Umoren, S. A. 2009, Int. J. Electrochem. Sci., 4, 863.
10. Obot, I. B. and Obi-Egbedi, N. O. 2010, Corros. Sci., 52, 198.
11. Madkour, L. H. and Zinhome, U. A. 2012, J. Corros. Sci. Eng., 15, 1.
12. Soltani, N., Salavati, H., Rasouli, N., Paziresh, M. and Moghadasi, A. 2015, Iran J. Anal. Chem., 2, 22.
13. Fajardo, V., Canto, C., Brown, B., Young, D. and Nesic, S. CORROSION 2008, paper no. 08333 (Houston, TX: NACE, 2008).
14. Chen, Y., Kiuchi, K., Chinone, K., Eguchi, M. and Momose, Y. J. 2001, Adhesion Sci. Technol., 15, 371.
15. Umoren, S. A., Obot, I. B., Ebenso, E. E., Okafor, P. C., Ogbobe, O. and Oguzie, E. E. 2006, Anti-Corros. Method. M., 53, 277.
16. Elgahawi, H., Gobara, M., Baraka, A. and Elthalabawy, W. 2017, J. Bio. Tribo. Corros., 3(55), 1.
17. Jain Kassim, M., Jian Ming, W., Hazwan Hussin, M. and Kang Wei, T. 2010, J. Corros. Sci. Eng., 13, 1.
18. Sliem, M. H., Afifi, M., Bahgat Radwan, A., Fayyad, E. M., Shibl, M. F., El-Taib Heakal, F. and Abdullah, A. M. 2019, Sci. Rep., 9(2319), 1.
19. Ajmal, M., Mideen, A. S. and Quraishi, M. A. 1994, Corros. Sci., 36, 79.
20. Kowczyk-Sadowy, M., Świsłocka, R., Lewandowska, H., Piekut, J. and Lewandowski, W. 2015, Molecules, 20, 3146.
21. Liu, K., Yan, L., Yao, G. and Guo, X. 2006, J. Chromatogr. B, 831, 303.
22. Świsłocka, R., Kowczyk-Sadowy, M., Kalinowska, M. and Lewandowski, W. 2012, Spectroscopy, 27, 35.
23. http://www.scribner.com/products
24. Brug, G. J., van der Eeden, A. L. G., Sluyters-Rehbach, M. and Sluyters, J. H. 1984, J. Electroanal. Chem., 176, 275.
25. Orazem, M. E. and Tribollet, 2008, B. Electrochemical Impedance Spectroscopy, John Wiley & Sons, New York, 225.
26. Metikoš-Huković, M., Babić, R., Grubač, Z. and Brinić, S. 1996, J. appl. Electrochem., 26, 443.
27. Titi, A., Mechbal, N., El Guerraf, A., El Azzouzi,·M., Touzani, R., Hammouti, B., Chung, I.-M. and Lgaz, H. 2018, J. Bio. Tribo. Corros., 4:22,1.
28. Khaled, K. F., Abdel-Rehim, S. S. and Sakr, G. B. 2012, Arab. J. Chem., 5, 213.
29. Škugor Rončević, I., Vladislavić, N., Buzuk, M., Buljac, M. and Lukin, A. 2020, Maced. J. Chem. Chem. Eng., 39, 167.
30. Atkins, P. W. 1986, Physical Chemistry, Oxford University Press, Oxford.
31. Mathammal, R., Jayamani, N. and Geetha, N. 2013, J. Spectrosc., 2013, 1.
32. Amitha Rani, B. E. and Basu, B. B. J. 2011, Int. J. Corros., 2012, 1.
33. Swisłocka, R., Kowczyk-Sadowy, M., Kalinowska, M. and Lewandowski, W. 2012, Spectroscopy, 27, 35.
34. Kowczyk-Sadowy, M., Świsłocka, R., Lewandowska, H., Piekut, J. and Lewandowski, W. 2015, Molecules, 20, 3146.